

Novel highest- T_c superconductivity in two-dimensional Nb₂C MXene

Zaheer Ud Din Babar, M. S. Anwar, Muhammad Mumtaz, Mudassir Iqbal, Ren-Kui Zheng, Deji Akinwande, Syed Rizwan**

Zaheer Ud Din Babar, Assoc. Prof. Dr. Mudassir Iqbal, Assoc. Prof. Dr. Syed Rizwan
Physics Characterization and Simulations Lab (PCSL), School of Natural Sciences (SNS),
National University of Sciences & Technology (NUST), Islamabad 44000, Pakistan.
Emails: syedrizwanh83@gmail.com, syedrizwan@sns.nust.edu.pk

Dr. M. S. Anwar
Department of Materials Science and Metallurgy, University of Cambridge, CB3 0FS
Cambridge, United Kingdom
Email: msa60@cam.ac.uk

Assoc. Prof. Muhammad Mumtaz
Materials Research Laboratory, Department of Physics, Faculty of Basic and Applied
Sciences (FBAS), International Islamic University (IIU) Islamabad 44000, Pakistan.

Prof. Dr. Ren-Kui Zheng
State Key Laboratory of High Performance Ceramics and Superfine Microstructure, Shanghai
Institute of Ceramics, Chinese Academy of Sciences, Shanghai 200050, China.

Prof. Dr. Deji Akinwande
Microelectronics Research Center, The University of Texas at Austin, Austin, Texas 78758,
United States.

Keywords: Nb₂CT_x MXene, 2D superconductivity, Spintronics, Transition temperature, Zero-field cooled

Currently, superconductivity in two-dimensional (2D) materials is a hot topic of research owing to their potential technological applications. Here, we report observation of superconductivity in a 2D Nb₂C MXene with transition temperature of 12.5 K, which is the highest transition temperature in MXene attained till now. We systematically optimized the chemical etching process to synthesize the Nb₂C MXene from its Nb₂AlC MAX phase. The X-ray diffraction (XRD) shows a clear (002) peak indicating the successful formation of MXene as well as a significant increase in the c-lattice parameter from 13.83Å to 22.72Å that indicates the delamination of Nb₂C MXene sheets as revealed by morphological study using scanning electron microscope. The Meissner effect is detected using superconducting quantum interference device (SQUID: Quantum design). Lower and upper critical fields as a

function of temperature follow the Ginzburg-Landau (GL) theory indicating the superconducting nature of the Nb₂C MXene. Strong-electron phonon interaction and the large density-of-states at Fermi level may cause the emergence of superconductivity at such a higher transition temperature which has theoretically been predicted for Mo₂C MXene. Our work is a significant advancement in the field of research and potential applications of 2D MXene.

Superconductivity in two-dimensional (2D) materials is fascinating in finding new Physics and is the foreground for many promising technological applications. Variety of astonishing physical phenomenon emerged in 2D materials, such as magnetism and superconductivity can revolutionize the field of spintronics and superconducting devices. Synthesis of new class of 2D materials, known as MXenes (M_{n+1}X_n), auctioned the possibility of magnetism in new 2D materials and their possible utilization in spintronics.¹⁻³ MXenes have attracted a lot of attention due to wealth of unusual physical and chemical properties as they were successfully derived from ‘MAX’ phase by selective etching of ‘A’ layers using hydrofluoric (HF) acid. The ‘A’ layer is chemically more reactive to fluoride containing acids and can be removed efficiently.⁴ Such 2D transition metal carbides (TMC’s) hold fascinating properties due to the coexistence of ionic, covalent and metallic bonds.⁵

Superconductivity in 2D materials hold a range of promising future applications thus, a lot of efforts are being made to synthesize 2D superconducting MXenes. Recently, 2D α -Mo₂C crystals were grown using chemical vapor deposition technique with crystal thickness in nanometer range.⁶ The superconductivity was observed in 2D α -Mo₂C MXene crystals with T_c around 3.6 K via resistivity versus temperature measurements. The suppression in T_c was observed with the increase of external applied magnetic field and the superconductivity was vanished completely at $H = 1.50$ T. Although the superconductivity phenomenon observed in α -Mo₂C MXene crystals is fascinating however, the main drawback is too low value of its T_c

(K). Further studied was carried out on Mo₂C crystals in order to explore its superconducting nature.^{7,8} They reported higher transition temperature $T_c \sim 8.02$ K. The authors however mentioned the small coherence length of 13.5 nm which was attributed to the presence of surface disorder. The enhanced superconducting properties of α -Mo₂C MXene crystals was proposed to be due to strain-induced coupling and increased lattice defects which were mainly associated with the Cu/Mo bilayer substrate and was not due to the intrinsic structure of MXene itself. The experimentally reported superconducting transition temperature in Mo₂C MXene is significantly lower than the theoretically predicted value of 13 K⁹ which demands more efforts to be done on this material. **Figure 1a** shows the summary of critical temperatures reported till date in the 3D-MAX and 2D-MXene.

In this work, we report a new two-dimensional powdered Nb₂C MXene superconductor with $T_c \sim 12.5$ K which is the highest value reported till date in 2D MXenes and is nearly equal to the predicted value of 13 K.⁹ We have systematically optimized etching process to convert bulk Nb₂AlC-MAX into a fine two-dimensional Nb₂C-MXene. The structural, morphological, magnetic and superconducting measurements were carried out in order to confirm its intrinsic superconducting nature. These results indicate that our as-synthesized powdered Nb₂C-MXene is superconducting indeed with highest superconducting properties in MXene 2D materials.

The structural and phase purity were characterized by X-ray diffractometer (XRD, Bruker, D8 Advance, Germany) using Cu-K α radiations. XRD spectra of powder Nb₂AlC-MAX and Nb₂C-MXene are shown in **Figure 2a**. XRD pattern of MAX phase is well-indexed according to hexagonal P6₃/mmc by JCPDF 00-030-0033.¹⁰ The disappearance of 100% intensity peak at 38.8° (00l) indicates the successful removal of 'Al' and conversion of MAX into two-dimensional MXene. In our results, peak at 12.9° is broadened and shifted to lower angle of 7.7° which shows a prominent increase in c-lattice parameter of hexagonally stacked layered structure after etching. The M-C bond has mixed characteristics of

metallic/ionic/covalent bonds while M-Al is metallic.¹¹ Due to weak nature of M-Al bonds than M-C bonds, the treatment of MAX phases in the presence of Fluoride containing acids at high temperature results in the removal of 'Al' layer. The replacement of metallic bonds among M-Al layers is altered by weaker hydrogen bond which grants the facile separation of the sheets after HF-treatment and water intercalation during washing. This suggests that difference in relative strengths of M-Al to M-C bonds allows the selective removal of 'Al' layer without disturbing M-C layers.¹² The elemental composition of the compounds were analyzed by energy dispersive X-ray (EDX) spectroscopy as shown in **Figure 2b**. Elemental mapping indicates that the 'Al' is much reduced in MXene compared to the MAX bulk part indicating our successful etching process. There are also some signatures of presence of O and F in MXene as functional groups which are unavoidable during etching process. The scanning electron microscope (SEM) images at different resolutions were recorded in field emission electron microscope (FESEM, VEGA3-TSCAN) operated at 20 KV. The SEM images of Nb₂AlC and Nb₂C-MXene are shown in **Figure 2(c & d)**, respectively. SEM images exhibit typical morphology of layered MXene with morphology similar to the exfoliated graphite.¹³ It can be seen that the MAX is composed of bulk-like closed sheets replaced by much wider sheets after chemical reduction. After etching under optimized temperature, the MXene sheets were considerably intercalated so as to be called the two-dimensional MXene sheets.

Since our Nb₂C MXene samples are in powder form so in order to study superconductivity, we investigated magnetic properties instead of electronic transport properties as the powder grains cannot be continuous to give realistic transport measurement. The magnetic measurements were carried out by using SQUID Magnetometer (Quantum Design, MPMS). The magnetization vs. temperature ($M(T)$) curves with field-cooled (FC) and zero field-cooled (ZFC) of as-synthesized Nb₂C MXene powder were carefully measured under applied magnetic fields of 10 mT, as shown in **Figure 3a**. Note that, before measurements, we removed residual magnetic field by resetting the superconducting magnet

of SQUID and oscillating magnetic field from 5 T to zero after linear increase. Diamagnetic transition in both, ZFC and FC curves is clearly observed that suggests the existence of superconductivity with onset transition temperature T_c^{onset} (K) ≈ 12.5 K. Expectedly, the difference between the ZFC-FC curves below T_c (see **Fig. 3a**) attributes the confinement of magnetic flux that results the flux pinning and the presence of substantial mixed state which asserts that the as-prepared Nb₂C-MXene is a type-II superconductor.¹⁴ There is a gradual decrease in magnetization upon decrease in the temperature that can be attributed to the formation of vortices below T_c (K). The broaden superconducting transition width (ΔT) in M-T curves is another indicative of vortex state which confirms type-II superconductor.

For more detailed confirmation of emergence of superconductivity in our samples, we studied Meissner effect by measuring magnetization loops ($M(H)$) at 5 K, 10 K and 20 K as shown in **Figure 3b**. Below T_c , the $M(H)$ loops reveal the superconducting behavior and at 20 K, strong paramagnetic behavior is clearly present. **Figure 3c** shows $M(H)$ loops measured from zero to maximum positive field to calculate the lower critical field H_{c1} and upper critical field H_{c2} . Both, H_{c1} and H_{c2} are monotonically decreasing with increase in temperature. We subtracted the paramagnetic contributions by removing linear increase at higher fields by presuming $M_d(H) = M_t(H) - M_p(H)$, where M_d , M_p and M_m are diamagnetic, paramagnetic and measured magnetizations, respectively. We calculate as $M_p = GH$, where G is the gradient at higher magnetic field and H is the applied magnetic field.

It can be seen that the width of M-H loop is much wider at 5K compared to other temperatures which can be attributed to the diamagnetic nature of Nb₂C sample and the improved grain connectivity. This width of M-H loop decreases with increase in measuring temperature which is consistent to the fact that the superconducting nature decreases at elevated temperatures. While moving from higher temperature to lower temperature after the onset of superconducting phase, the vortices come into action that induce strong superconducting diamagnetism at low temperatures. Moreover, it can also be observed that

the diamagnetic nature of the material changes to paramagnetic upon increasing the temperature above critical temperature. The vortices at low temperature are stationary and magnetic flux pinning among them becomes stronger, exhibiting strong superconductivity. Further increase in temperature may destabilize the grain connectivity, consequently destroying the flux pinning among the grains at temperature above T_c hence, the material comes to the normal state.¹⁵ The enhanced vortex dynamics at elevated temperatures above T_c results in destruction of magnetic flux configurations causing lesser flux pinning among the grains thus, the material turns to normal (paramagnetic) state from the superconducting state.

The variation of H_{c1} and H_{c2} as a function of temperature T is shown in **Figure 3d**. The solid lines show the fitting of H_{c1} and H_{c2} according to the Ginzburg-Landau (GL) theory for superconductors as follows: $H_{c1}(T) = H_{c1}(0)[1-(T/T_c)^2]$ and $H_{c2}(T) = H_{c2}(0)[1-(T/T_c)^2]$, respectively.¹⁶ The values of H_{c1} and H_{c2} were calculated from experimental data as illustrated in **Figure 3c**. The calculated values are well-fitted to theoretical predictions of well-known Ginzburg-Landau theory and phase diagram of **Figure 3d** translates the characteristic behavior of type-II superconductor with well-defined normal (line above H_{c2}), vortex states (between H_{c1} and H_{c2}) and superconducting states (below fitting line of H_{c1}). We also estimated the superconducting coherence length (ξ_s) using the GL expression $H_{c2}(0) = \varphi_0 / 2\pi\xi_s^2$, where, φ_0 is the flux quantum and $H_{c2}(0)$ is estimated with extra polation of data presented in **Figure 3d**. It yeilds that $\xi_s = 25$ nm, which is not significantly different than that of $\text{Mo}_2\text{C MXene}$.¹⁷

Now, we discuss the relatively higher T_c of our samples by presuming that it may come from some imurity phases (if any) that may present in our samples such as Nb, NbC, NbAlC, Al and Nb_2C (3D), as well. It is well know that T_c of Nb, NbC and Al is 9.2 K, 9 K and 1.2 K, respectively. Superconductivity was also observed in NbAlC with T_c of 0.44 K. Furthermore,

G. F. Hardy *et al.* prepared 3D hexagonal, non-MXene Nb₂C samples (c -LP = 4.970Å) and reported the superconductivity with $T_c = 9.18$ K.¹⁸ Note that none of the above materials were in two-dimensional phase. Our Nb₂C sample is a 2D MXene with much higher c -lattice parameter (c =LP ~ 22.7Å) and $T_c \sim 12.5$ K. It suggests that superconductivity in our samples is mainly emerged due to the intrinsic two-dimensional structure of Nb₂C MXene. Interestingly, T_c of our samples is almost close to the theoretical prediction of T_c for Mo₂C MXene which suggests that high T_c in our sample is due to the 2D structure itself and not due to any impurity phase. The absence of impurity phases discussed above were also confirmed by XRD results and can safely be ruled out.

The first principles density functional theory (DFT) calculations of Mo₂C monolayer predict that the T_c can be enhanced to 13 K depending upon the electron-phonon coupling strength.⁹ Although the theory predicted T_c for Mo₂C MXene but we believe it could be generalized to other MXene family with $n=1$ in its general formula 'M_{n+1}X_n'. These calculations show that several bands have crossed the Fermi level with substantially higher density-of-states (DOS), which can enhance T_c . It was also pointed out that the prerequisite for superconductivity in all considered monolayers is the presence of metallic elements. Fortunately, the superconducting transition temperature in our Nb₂C MXene system is very close to the predicted value of 13 K for Mo₂C system. Moreover, in our system, all elements are metallic in nature which fulfills the condition necessary for the occurrence of superconductivity. Therefore, it can be understood that the electron-phonon interaction in our Nb₂C MXene system is very strong and we can predict that the DOS above the Fermi level will be much higher compared to all other 2D MXenes.

Critical current density (J_c) is one of the important parameters of superconductors from applications point of view. The Bean's model can be used to calculate the J_c using parameters taken from $M(H)$ loops measured at different temperatures 5 K and 10 K¹⁹⁻²¹.

Since, the sample was placed in a cylindrical glass voil hence, Bean's model for cylindrical sample was used and is given by: ²²

$$J_c = 30 \frac{\Delta M}{d}$$

Where, $\Delta M = [|M_+| - |M_-|]$ measured in emu/cm³ and 'd' is the diameter of the cylinder in cm. As the dimension of sample is same so, J_c is directly proportional to ΔM (i.e. width of the $M(H)$ loop). The J_c versus applied magnetic field (H) at two different temperatures (5 K and 10 K) is drawn in **Figure 4**. It can be seen from these graphs that J_c was decreased with increasing temperature and also with increasing applied magnetic field.²³

Conclusion

In summary, we have successfully synthesized high quality Nb₂C 2D MXene sheets under optimized conditions. The XRD pattern shows a significant increase in the lattice parameters indicating large intercalation of MXene sheets. The $M(T)$ and $M(H)$ measurements indicate the existence of superconductivity in as-synthesized MXene powder with high $T_c = 12.5$ K. The fitting of critical fields (H_{c1} and H_{c2}) as a function of temperature according to GL theory, also confirms the characteristic behavior of type-II superconductivity. It is worth paying attention that, to our knowledge, this is the first study on the superconductivity of as-prepared MXene (Nb₂C-powder in present case) which shows highest $T_c = 12.5$ K, which is close to the theoretically predicted value of 13 K. The possible reasons for such a higher T_c in Nb₂C MXene maybe strong-electron phonon interaction as well as the presence of higher density-of-states at the Fermi level. This work is a significant development to explore the physical properties exhibited by 2D materials particularly the MXenes which offer unique potential for future applications.

Experimental Section

The materials used for etching process includes Hydrofluoric acid solution (50 wt. % in H₂O, $\geq 99.99\%$), Niobium Aluminum Carbide Powder (Nb₂AlC, purity 90-95 %, 200mesh), de-

ionized water, absolute ethanol. In order to obtain the two-dimensional sheets of MXene, etching was performed to selectively remove aluminum (Al) from Nb₂AlC-MAX Phase. The Nb₂AlC powder was added in 50% HF (sigma Aldrich) in the ratio (1:10) at room-temperature (RT) in a Teflon beaker and was continuously stirred for 90 hours by Teflon-coated magnetic stirrer.²⁴ Etching of our MAX was not successfully done at such conditions. Then, we performed a systematic study of etching process at optimized time of 40 hrs and at varying temperature (45°C - 85°C) to get our final product. After HF treatment, the suspension was washed several times by deionized water and centrifuged at 3500 rpm for 5 minutes until the pH reached to 7. The HF selectively removes the Al, which, in succession replaced by F, O and/or OH. Each time, the supernatant was removed and settled powder was removed from centrifuge bottles using ethanol and dried at room-temperature.

The schematic of this etching process is shown in **Figure 1b** which gives a physical insight towards sheets separation upon HF treatment and separation of finally obtained sheets after washing and drying. The yield here is addressed as the weight of MXene/ MAX times 100 ($W_{\text{MXene}}/W_{\text{MAX}} \times 100$), was, almost 100% and resultant MXene was obtained in maximum amount without prominent losses. For magnetic measurement the powdered sample was put into a capsule mounted in a tube. Before starting the measurement, the system was calibrated by using an oscillatory field in order to eliminate the entire stray fields among the coils, so the real magnetic behavior of the sample could be observed.

Acknowledgements

The authors are thankful to Higher Education Commission (HEC) of Pakistan for providing research funding under the Project No.: 6040/Federal/NRPU/R&D/HEC/2016 and HEC/USAID for financial support under the Project No.: HEC/R&D/PAKUS/2017/783.

References

- [1] Naguib, M.; Kurtoglu, M.; Presser, V.; Lu, J.; Niu, J.; Heon, M.; Hultman, L.; Gogotsi, Y.; Barsoum, M.W. *Adv. Mater.* **2011**, 23, 4248.
- [2] M. Iqbal, J. Fatheema, M. Rani, R.-K. Zheng, S. A. Khan, Syed Rizwan, **2019**, *preprint*: arXiv:1907.12588 [cond-mat.mes-hall]
- [3] Ayesha Tariq, S. Irfan Ali, Deji Akinwande, Syed Rizwan, *ACS Omega* **2018**, 3, 13828.
- [4] Naguib, M., Mashtalir, O., Carle, J., Presser, V., Lu, J., Hultman, L., Gogotsi, Y., Barsoum, M.W. *ACS Nano* **2012**, 6, 1322.
- [5] Oyama, S.T. *The chemistry of transition metal carbides and nitrides*, Springer, Dordrecht. **1996**.
- [6] Xu, C., Wang, L., Liu, Z., Chen, L., Guo, J., Kang, N., Ma, X.L., Cheng, H.M. Ren, W. *Nature Mater.* **2015**, 14, 1135.
- [7] Wang, L., Xu, C., Liu, Z., Chen, L., Ma, X., Cheng, H.M., Ren, W., Kang, N. *ACS Nano*, **2016**, 10, 4504.
- [8] Zhang, Z., Gedeon, H., Cheng, Z., Xu, C., Shao, Z., Sun, H., Li, S., Cao, Y., Zhang, X., Bian, Q. Liu, L. *Nano Lett.* **2019**, 19, 53327.
- [9] Lei, J., Kutana, A., Yakobson, B.I. *J. Mater. Chem. C*, **2017**, 5, 3438.
- [10] Peng, C., Wei, P., Chen, X., Zhang, Y., Zhu, F., Cao, Y., Wang, H., Yu, H., Peng, F. *Cer. Intl.* **2018**, 44, 18886.
- [11] Sun, Z., Music, D., Ahuja, R., Li, S., Schneider J.M. *Phys. Rev. B*, **2004**, 70, 092102.
- [12] Naguib, M., Mochalin V. M., Marsoum M. W., Gogotsi Y. *Adv. Mater.* **2014**, 26, 992.
- [13] Viculis, L.M., Mack, J.J., Mayer, O.M., Hahn, H.T., Kaner, R.B., *J. Mater. Chem.* **2005**, 15, 974.
- [14] Takano, Y., Takeya, H., Fujii, H., Kumakura, H., Hatano, T., Togano, K., Kito, H. Ihara, H. *Appl. Phys. Lett.* **2001**, 78, 2914.
- [15] Joshi, A.G., Pillai, C.G.S., Raj, P., Malik, S.K. *Solid State Comm.* **2001**, 118, 445.

- [16] Tiwari, B., Goyal, R., Jha, R., Dixit, A. and Awana, V.P.S., *Superconductor Sci. Tech.* **2015**, 28, 055008.
- [17] Geng, D., Zhao, X., Li, L., Song, P., Tian, B., Liu, W., Chen, J., Shi, D., Lin, M., Zhou, W. Loh, K.P. *2D Mater*,2017, (011012), 2053.
- [18] Hardy, G.F. Hulm, J.K. *Phys. Rev.* **1954**, 93, 1004.
- [19] G. Kirat, O. Kizilaslan, M.A. Aksan, *Ceram.Intl.* **2016**, 42, 15072.
- [12] C.P. Bean, *Phys. Rev. Lett.* **1962**, 8, 250.
- [21] M. Mumtaz, Mirza Hassan Baig, M. Waqee-ur-Rehman, M. Nasir Khan, *Physica B* **2018**, 537, 283.
- [22] V.P.S. Awana, Rajeev Rawat, Anurag Gupta, M. Isobe, K.P. Singh, Arpita Vajpayee, H. Kishan, E. Takayama-Muromachi, A.V. Narlikar, *Solid State Comm.* **2006**, 139, 306.
- [22] S. Farhadi, K. Pourzare, S. Sadeghinejad, *J. Nanostruct. Chem.* **2013**, 3, 16.
- [24] Naguib, M.; Halim, J.; Lu, J.; Cook, K.M.; Hultman, L.; Gogotsi, Y.; Barsoum, M.W. *J. Am. Chem. Soc.* **2013**, 135, 15966.

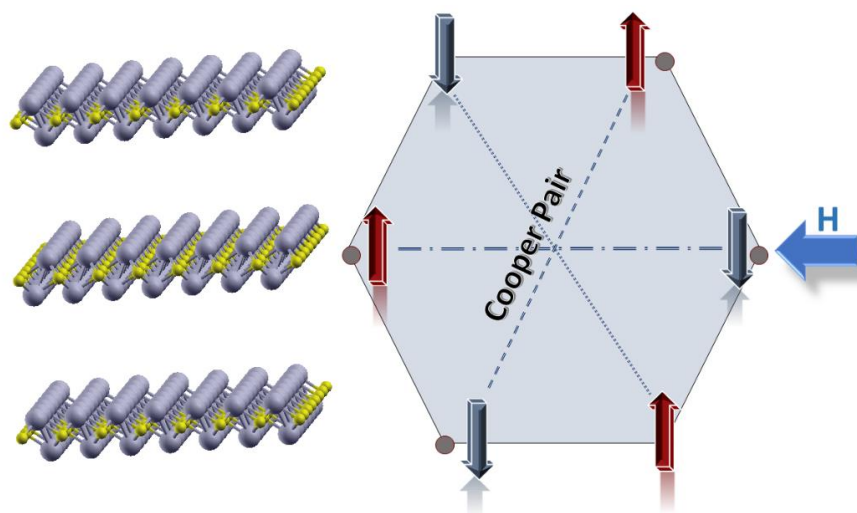


Table of Content (TOC) – Art File

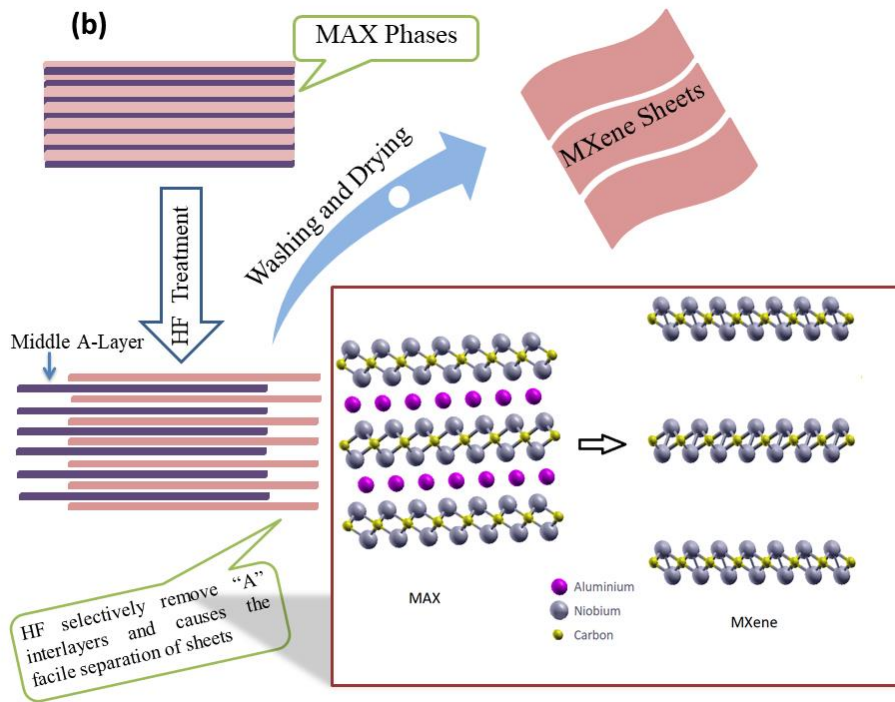
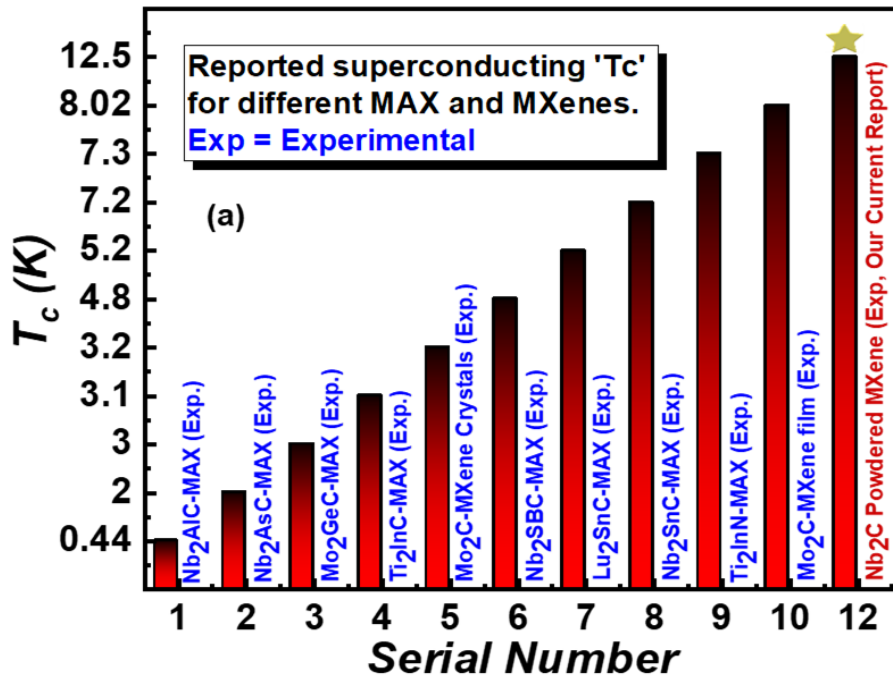


Figure 1. (a) Summary of superconducting transition temperature of various MAX (3D) and MXene (2D) superconductors reported till date. (b) Schematic of chemical etching protocol of synthesis of MXene 2D sheets from MAX phase.

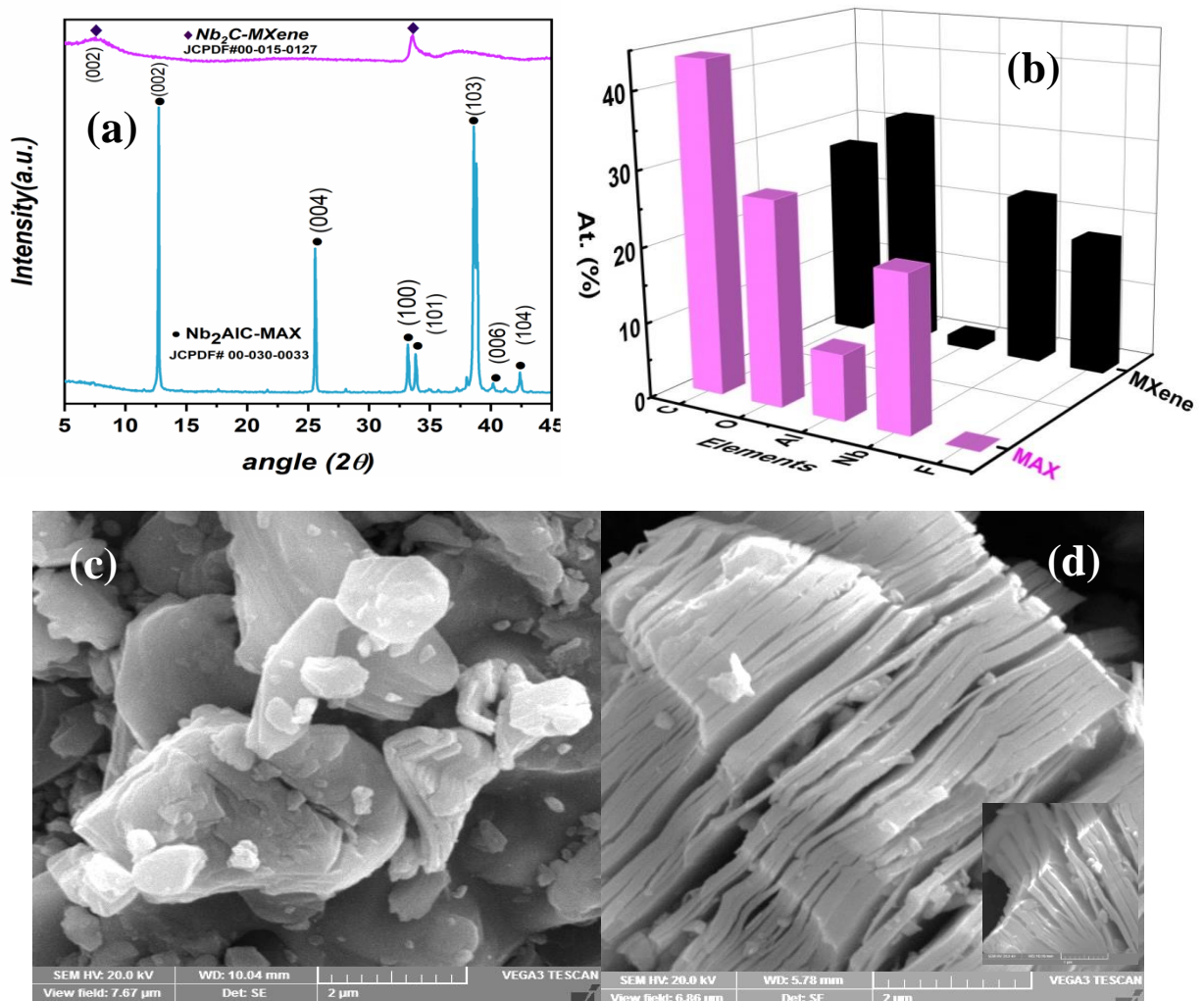


Figure 2. (a) X-ray diffraction of Nb_2AlC MAX and MXene before and after treatment, respectively, indicating the removal of 'Al' (b) energy dispersive X-ray (EDX) spectrum of MAX and MXene which shows significant decrease in 'Al' percentage after HF treatment (c) Scanning Electron Microscopy (SEM) shows lamellar structure of MXene.

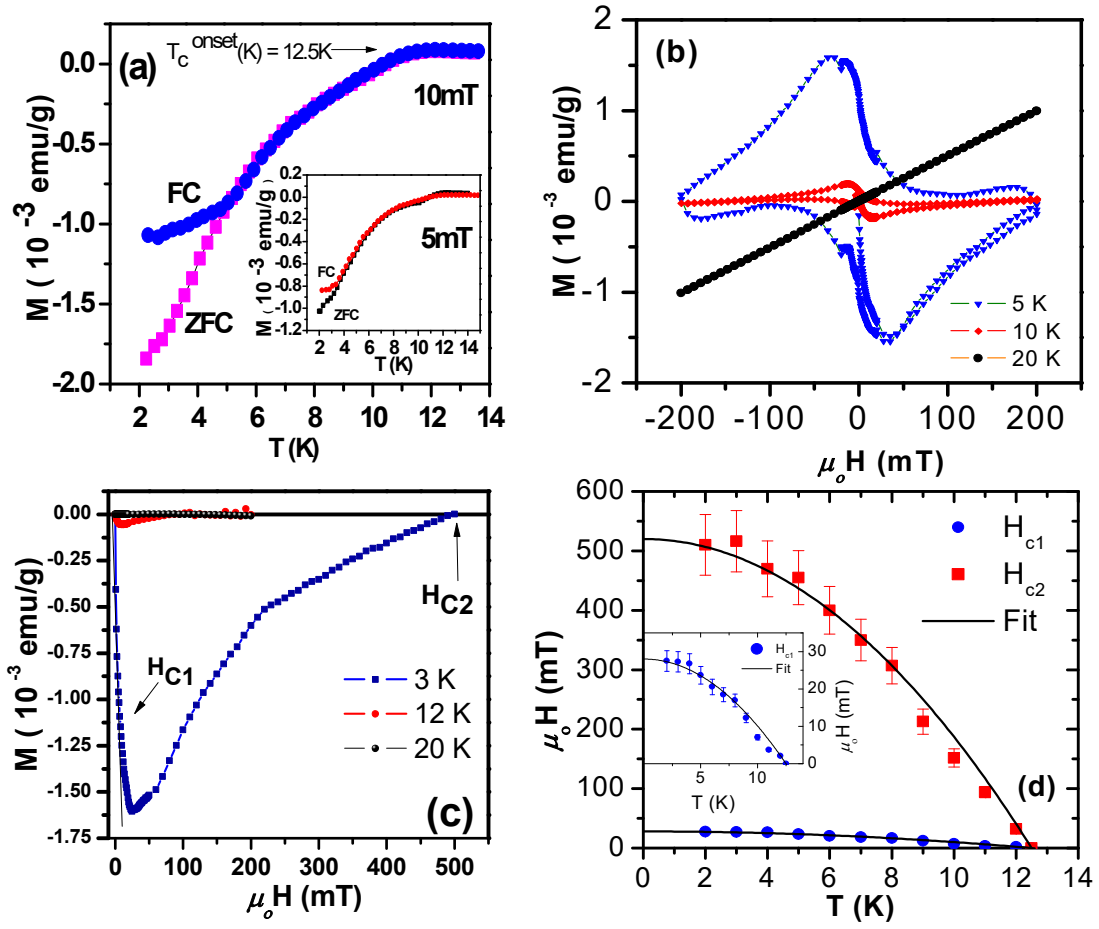


Figure 3. (a) zero-field-cooled (ZFC) and Field-cooled (FC) curves indicating T_c^{onset} (K) =12.5 K (b) M-H loops (M vs. H) shows typical loops Type-II superconductor (c) Lower critical field (H_{c1}) and Upper critical field (H_{c2}) depicts the characteristic fields of Type-II superconductor (d) fitting of experimentally calculated H_{c1} and H_{c2} as a function of temperature T/T_c in accordance with GL theory of superconductivity.

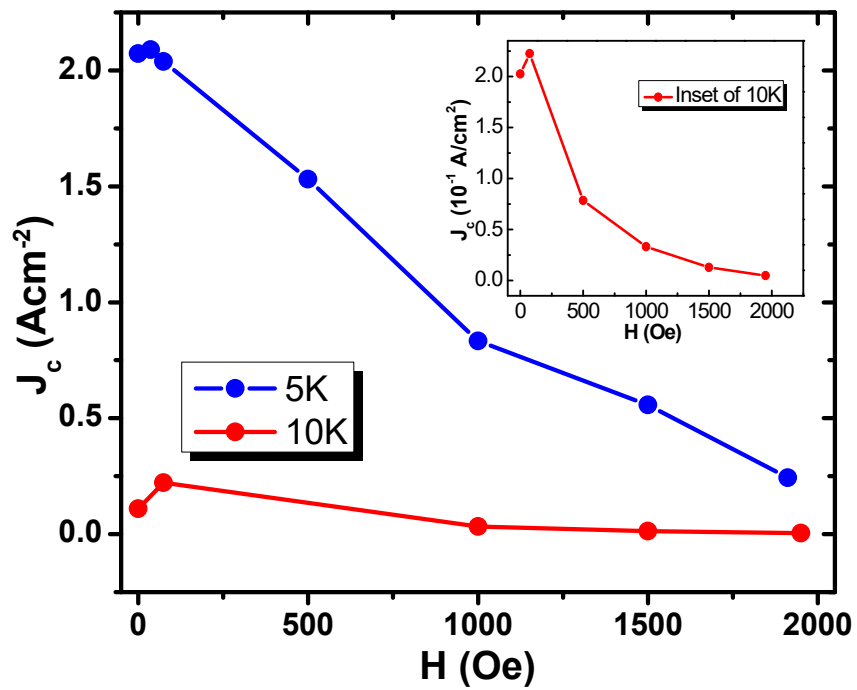


Figure 4. Calculated critical current density J_c versus applied magnetic field at 5 K and 10 K: inset is the zoom-version of the same at 10 K.